ORIGINAL ARTICLE

Transcriptomic Analysis of the Liver and Brain in Grass Carp (*Ctenopharyngodon idella*) Under Heat Stress

Wei Zhang[1] · Xiaoyan Xu[1,2] · Jiale Li[1,2] · Yubang Shen[1,2]

Abstract

Temperature is a major environmental factor that influences growth, development, metabolism, and physiological performance in fish. Grass carp (*Ctenopharyngodon idella*) is a highly productive fish in freshwater culture. To understand the molecular mechanism of grass carp under heat stress, we used RNA-Seq to analyze the liver and brain transcriptome of 12 libraries constructed from high-temperature (36 °C) and control (28 °C) groups. We obtained 42.49 and 42.57 GB of clean data from six liver and six brain libraries, respectively, and identified 2,534 genes that were differentially expressed in liver tissue and 1622 in brain tissue ($P < 0.05$). According to KEGG analysis, significant differences occurred in the expression of genes involved in metabolic and immune pathways, such as the cAMP signaling pathway, apoptosis, calcium signaling pathway, lipid metabolism, and protein processing in endoplasmic reticulum and peroxisome proliferator-activated receptor signaling pathways. This study revealed that high temperature enhanced lipid metabolism, reduced fatty acid synthesis, and disrupted the immune system of grass carp. These results investigated the molecular regulation of heat stress in grass carp and provided valuable information for the healthy culture of grass carp under high temperatures.

Keywords Grass carp · Transcriptome · High temperature · Metabolism · Immune

Introduction

Temperature is a critical environmental factor that severely affects the physiological state of fish (Mahanty et al. 2017), and, as an eco-physiological variable, is associated with metabolic processes that characterize the basic life history of animals with variable temperatures (Brett 2015; Huey and Stevenson 2015). By disrupting internal homeostasis, environmental stress can affect biological functions detrimentally. Heat stress is a relatively common environmental stressor. A high temperature can have several detrimental effects on fish, which can affect respiratory metabolism and growth (Handeland et al. 2008), decrease

✉ Jiale Li
  jlli2009@126.com

✉ Yubang Shen
  ybshen@shou.edu.cn

1   Key Laboratory of Freshwater Aquatic Genetic Resources, Ministry of Agriculture and Rural Affairs, Shanghai Ocean University, Shanghai 201306, China

2   Shanghai Engineering Research Centre of Aquaculture, Shanghai Ocean University, Shanghai 201306, China

immunity, increase the risk of death (Verma et al. 2007; Zhao et al. 2017), decrease antioxidase activities (Bo et al. 2010), activate apoptosis (Zhi et al. 2019), and disrupt other physiological processes. Recent studies have found that liver tissue under high-temperature stress could inhibit protein synthesis, decrease fatty acid synthesis, and weaken carbohydrate metabolism in juvenile grass carp (Huang et al. 2022). Several differentially expressed genes (DEGs) with critical roles in immune function, including heat shock proteins (HSPs), complement system, PRRs, cytokines, antigen processing and presentation, cell adhesion molecules, apoptosis, and keratins are known to influence the regulatory mechanism of immune responses to high temperature in grass carp. Some studies have been discussed through the transcriptome of spleen tissue the effect of high temperature to immune response against bacterial (Yang et al. 2016).

RNA-seq is a method for transcriptome analysis using deep sequencing technology (Sangwan et al. 2013). Because high temperature affects the expression of many genes in fish, transcriptomic techniques can be applied to resolve the complex molecular regulatory mechanisms of organisms under temperature stress (Jeffries et al. 2013).

Transcriptomic analyses under temperature stress have been carried out in various fish species, such as juvenile blunt snout bream (*Megalobrama amblycephala*) (Bing et al. 2019), Nile tilapia (*Oreochromis niloticus*) (Mahmoud et al. 2020), common carp (*Cyprinus carpio*) (Iranshahi et al. 2011), and rainbow trout (*Oncorhynchus mykiss*) (Huang et al. 2018). Heat stress is a complex adaptive response in an organism, and the brain and liver are the two most important organs involved in this response. The transcriptome analysis of nutrient metabolism in grass carp (*Ctenopharyngodon idella*) under heat stress has been reported. The liver is a major metabolic organ, which performs important physiological functions such as metabolism, excretion, and detoxification (Sun et al. 2018). At the same time, it was found to be a major metabolic organ under high temperatures (Zhao et al. 2021). The brain is an organ that regulates the biological function of fish and is also closely related to temperature response (Zhou et al. 2020). It can further regulate the liver by regulating the function of the pituitary gland. Heat stress will have complex effects on all aspects of fish, so it is urgent to understand the complex molecular regulation of grass carp under high temperatures.

Grass carp is an important farmed freshwater fish species in China (Shen et al. 2019; Guo et al. 2022), and its production in farming ranks among the top in global freshwater fisheries (Wenning 2020). With the increase in global warming and persistent summer heat (Edenhofer et al. 2014), farmed grass carp have serious disease problems due to pathogenic bacteria and stress (Liu et al. 2010), resulting in reduced temperature adaptation and weakened resistance to diseases (Yang et al. 2016). Therefore, the application of molecular biological research on the regulatory mechanism of grass carp under high-temperature stress and the screening of relevant functional genes are essential for the healthy culture of grass carp under high temperatures (Shen and Yue 2018).

The aim of this study was to investigate the molecular regulatory mechanisms of grass carp under high temperature in brain and liver transcriptomes, and to identify the DEGs and important pathways involved in the relevant regulatory processes. This study laid the theoretical foundation for analyzing the complex molecular mechanism of grass carp under high temperature stress and will have significance as a reference for the healthy culture of grass carp under high temperatures.

Materials and Methods

Ethics Statement

All experiments were performed according to the Guidelines for the Care and Use of Laboratory Animals in China. The animals used in the present study were cultured and sacrificed following the terms for the use of animals approved by the Institutional Animal Care and Use Committee at the Shanghai Ocean University (Shanghai, China) (approval number SHOU-DW-2018−026). All efforts were made to minimize suffering. Before dissection, fish were anesthetized with 3-aminobenzoic acid ethyl ester methane sulfonate (MS-222; Sigma-Aldrich, St. Louis, MO, USA) to minimize suffering.

Experimental Animals and Thermal Stress

We obtained healthy grass carp juveniles (average body length 82.712 ± 9.808 mm, weight 11.241 ± 3.727 g) from a ZhuJiang population provided by Wujiang National Farm of Chinese Four Family Carps, Jiangsu Province, China, and cultured at Hangzhou Aquaculture Research Institute (Hangzhou, China). Before the experiment, the grass carp were temporarily cultured in a cement pond for 2 weeks at an ambient temperature of 28 ± 2 °C and 180 grass carp of similar size were randomly selected. The experimental fish were evenly divided into two groups, a high temperature group (ZJ-1) and a control group (ZJ), and each group was performed in triplicate. The control group was cultured at 28 °C for 21 days, and the high-temperature group was cultured at a heating rate of 1 °C/12 h until the temperature reached 36 °C and maintained for 21 days. During the experiment, fish were fed twice daily with commercial pellet feed from Tongwei Co. (Chengdu, China).

Sample Collection and RNA Preparation

The fish were closely monitored for signs of stress. After 21 days, nine fish (three repetitions per group) were randomly selected from each experimental group and anesthetized in MS-222 (100 mg/L). Liver and brain tissues from the high-temperature treatment group (ZJ-GZ1 and ZJ-N1) and the control group (ZJ-GZ and ZJ-N) were immediately removed from the fish of each tank at the two temperatures, and stored quickly at −80 °C until total RNA extraction for RNA-Seq analysis.

RNA Isolation, Library Construction, and Sequencing

Total RNA was isolated from liver and brain tissues using TRIzol reagent (Invitrogen, Carlsbad, CA, USA) following the manufacturer's procedure. The total RNA quantity and integrity were analyzed by a Qubit RNA assay kit (Life Technologies, Carlsbad, CA, USA), and a Bioanalyzer 2100 RNA Nano 6000 assay kit (Agilent Technologies, Santa Clara, CA, USA) with RIN > 7.5, to meet the experimental requirements. After total RNA was extracted,

magnetic beads with oligo (dT) were used to enrich the mRNA. Then, the mRNA fragment was reverse transcribed into cDNA with random primers. Second-strand cDNA was synthesized with dNTP, DNA polymerase I, and RNase H and then subjected to 3′-end repair, a poly(A)-tail was ligated to the sequencing linker. Finally, PCR amplification was performed. The constructed libraries were quantified with the Agilent 2100 Bioanalyzer and sequenced with an Illumina HiSeq X Ten sequencer (San Diego, CA, USA) to generate 150 base pair (bp) double-end data.

Data Processing, Assembly, and Differential Expression Analyses

A large number of double-ended sequencing data were obtained through the Illumina platform. In view of the data error rate influence on the results, Trimmomatic (Bolger et al. 2014) was used to preprocess the quality of the original data, and the number of reads in the whole quality control process was summarized statistically. Hisat2 (Kim et al. 2015) was used to conduct sequence alignment between cleaned reads and the specified reference genome to obtain the location information on the reference genome or genes, as well as the sequence characteristic information of the sequenced samples. The known reference gene sequences and annotation files were used as a database, and a sequence similarity comparison method was used to identify the expression abundance of each protein-coding gene in each sample. Htseq-count was used to obtain the number of reads compared to protein-coding genes in each sample (Anders et al. 2015). DESeq2 (Love et al. 2014) was used to standardize the count number of each sample gene (BaseMean value was used to estimate the expression level), calculate the multiple of difference, and the negative binomial distribution (NB) test was used to test the significance of the difference. Finally, the differential protein-coding genes were screened according to the difference in multiple and significance test results (|fold-change|≥ 2 and P value < 0.05).

GO enrichment analysis (http://geneontology.org/) was performed on the DEGs obtained to describe their functions (combined with GO annotation results). KEGG is a major public database of molecular pathways. Pathway analysis was carried out on differential protein-coding genes using the KEGG database (http://www.genome.jp/kegg/), and the significance of differential gene enrichment in each pathway item was calculated using a hypergeometric distribution test. GO/KEGG enrichment analyses were performed using the ClusterProfiler R package.

Validation of DEGs

The response of genes to high temperature stress was used to select 24 differential genes in related pathways from the liver and brain tissues, and these were verified and analyzed by quantitative real-time PCR (qRT-PCR). To evaluate the reliability of the RNA-Seq method to identify the differential genes, the total RNA used in quantitative experiments was the same as that used in sequencing. Primer3.0 (Wang et al. 2019) was used to design primers for different genes (Table 1). CFX96™ Real-Time fluorescence quantitative PCR detection system (BioRad, Hercules, CA, USA) and SYBR Green master mixture (Takara, Shanghai, China) were used for qRT-PCR experiments. The 20 µL reaction system consists of the following components: 1.6 µL cDNA produced by reverse transcription, 0.8 µL of each primer (10 µm/L), 10 µL of TB Green™ Premix ExTaq (Takara), and 6.8 µL of RNase free H$_2$O. The PCR amplification procedure is as follows: one cycle at 95 °C for 30 s; 35 cycles at 95 °C for 5 s, 60 °C for 30 s, and 72 °C for 1 min; and 1 cycle at 72 °C for 3 min. The $2^{-\Delta\Delta Ct}$ method was used to calculate the relative expression levels of different genes at different sites. The 18 s rRNA gene was used as an internal control and three biological replicates were performed for each sample. SPSS19.0 (SPSS Inc.) was used for statistical analysis, and a one-way ANOVA and t-test were used to determine the significance of the difference. A p value of < 0.05 was considered statistically significant.

Results

Preliminary Analysis of the Liver and Brain Transcripts

Twelve experimental cDNA libraries were constructed from the liver and brain tissues of the high-temperature (ZJ-1) and control (ZJ) groups. Through the Illumina HiSeq™ 2000 platform, a total of 584,782,480 clean reads and 85.24 GB of clean data were obtained from the 12 samples. The effective data of each sample ranged from 6.83 to 7.33 GB. The Q30 bases in the transcriptome data ranged from 90.81 to 94.66% and the average GC content was 46.42% (Table 2). By comparing reads to the reference genome, the genome alignment of each sample was obtained, and the alignment rate was 95.11–95.74%. After the counts were obtained by comparison, the protein-coding genes were filtered to remove the genes with zero reads. The number of genes detected in each sample is shown in Table 3. The expression of protein-coding genes was calculated using fragments per kilobase per million reads (FPKM) (Roberts et al. 2011). This could

Table 1 Primers used to verify transcriptome data. Selected differentially expressed genes

Gene name	Primers
GLRB	F:C TTCAGCATCGTCGGCTCTC R:AGCAGTGCCGACTTCAATGG
GRIA2	F:CCAAATGGCGCATCAACGTC R:AGAGCGCTGGTCTTCTCCTT
BCL2L1	F:CTGCGTTATTCCCGAGVGTT R:CGCGGAACACCTCATCCATC
SLC22a5	F:AGACACCGAGTGGACATCGT R:AGCCGTCCATACAGGCTTCT
Abca1	F:CTGCAGCCGGTGATGAAGTT R:TGTGAGCGAGGGAGGTAAGG
Asah1	F:CGCAGAACACCGGCAATGA R:GGCGTGCATGGATTTGGACA
rest	F:TCTGAGTCATCGCCAGCACG R:TCAGCCGCACCATTTACCAC
Faf2	F:GAGTTCTGCCGAGCCACATT R:CACTCGGTAACCCTCTGGCT
GPX3	F:GCCAAACGTCACCCTCATGT R:CCTACACCTGGGCTGGGTAT
Anxa6	F:GGTCTCTCGCGCTGAGATTG R:CAGCAGGGTGCGTTTGTACT
SLC22a1	F:TGCTGCTCGCATTTGTGCTA R:AGCGCGTCAAACTTCACACA
Fgfbp1	F:TGTAGCAAAGCCCGCAACAT R:GCTCCTGCACATACTGGCTT
mad2l2	F:GCTGCTGAGAGCAGTGATCC R:TTCTTGTGGCGGCTTCCCTA
Wee2	F:GCCTCAGACAGGGTGAGCTA R:AGCTCCTTGCGAAGCTGTTC
ZDHHC2	F:TCTGCCTGATACCCAAGCCA R:GCAGACAAGCCAGCAGTGAT
Ebp	F:CTATTGGCCACGCAACCTGT R:TGCTCCCAGACACTTTACGC
abhd8	F:GCAAAGACGACCAGCGTTGT R:CTGGCTTCACCTCCACGAAC
GDF9	F:AGAGCCACGCAAGGTAGGAT R:TGACTCCCACAACGTGGACT
ddit4l	F:ATGTCCGCCAGGAGAGTTCA R:GGACGCACGTCTTCTCCTTC
GFRA2	F:CCGGTGTTCCCTGGGACTAT R:AGCGCATGAGGTTGTTCTGG
trpt1	F:TCAGGGCCTCAGCAGAATGA R:CAGCACACCGTTCTCTGACC
ADAM19	F:AGTGCATCCTTCCTGCAAGC R:CAATCACAGGCCCACTGTCC
Prss23	F:TGTCCGGTGGAGGATGAGTC R:AGCGAACAGCCACGTTGTAG

eliminate the influence of protein-coding gene length and the difference in the amount of sequence on the expression of the calculated protein-coding gene, which is either high or low (Fig. 1).

Analysis of DEGs

A total of 4156 DEGs were identified by differential expression analysis from the high-temperature treatment (ZJ-1) and the control (ZJ) groups (Fig. 2a). In liver tissue, 2534 DEGs (Table S1) were identified between the ZJ-GZ1 and ZJ-GZ groups, including 974 upregulated genes and 1560 downregulated genes. In brain tissue, 1622 DEGs (Table S2) were identified between the ZJ-N1 and ZJ-N groups, among which, 1027 genes were upregulated and 595 were downregulated. Venn diagram in Fig. 2b showed statistics of the number of common and unique differentially expressed genes among different comparison groups. A volcano map was used to understand the overall distribution of DEGs (Fig. 2c). The results showed that the fold change of DEGs generally ranged from -10 to -1 and 1–10. More differential genes were identified in the liver than in brain tissues. Similar to the volcano map, the results in the heat map also showed that there were more upregulated DEGs in the ZJ-N group and more downregulated DEGs in the ZJ-GZ group (Fig. 2d).

Gene Ontology and KEGG Analysis of DEGs

GO enrichment analysis was performed for DEGs, and their functions were described (combined with GO annotation results) and classified into three broad categories: biological process, cellular component, and molecular function. GO entries with more than two different genes in the three categories were identified, and 10 items were sorted in descending order according to the corresponding $-\log10\ p$ value of each entry. The top 30 items in the GO enrichment analysis can be found in Fig. 3. The results showed that the top three terms with the most enriched genes between the ZJ-GZ1 and ZJ-GZ groups were rRNA processing (GO: 0006364), cell junction (GO: 0030054), and ATPase binding (GO: 0005524). Between ZJ-N1 and ZJ-N, the top three terms with the most enriched genes were cholesterol biosynthetic process (GO: 0006695), condensing complex (GO: 0000796), and hormone activity (GO: 0005179). GO is generally divided into three levels according to the functional classification. Figure 4 showed the comparison of upregulated and downregulated DEGs at GO level 2. In the comparison between experimental group ZJ1 and control group ZJ, cellular process, biological regulation, and metabolic process were the top three terms with the most enriched genes in biological process; organelle, macromolecular complex, and membrane were the most enriched terms; in cellular component; and binding, catalytic activity, and transporter activity were the most enriched terms in molecular function.

Table 2 Summary of the grass carp transcriptome data.Q30: percentage of nucleotides with a quality value > 30 in reads

	Raw read (Mb)	Raw bases (Gb)	Clean reads (Mb)	Clean bases (Gb)	Valid bases	Q30	GC
ZJ-N-1	48.53	7.28	47.72	6.95	95.42%	94.37%	45.13%
ZJ-N-2	49.91	7.49	49.07	7.14	95.35%	94.54%	44.79%
ZJ-N-3	48.81	7.32	47.9	6.98	95.39%	93.70%	44.78%
ZJ-N1-1	50.27	7.54	49.46	7.19	95.39%	92.51%	46.43%
ZJ-N1-2	48.59	7.29	47.8	6.96	95.51%	92.82%	46.33%
ZJ-N1-3	50.82	7.62	50.05	7.27	95.40%	92.72%	46.20%
ZJ-GZ-1	47.61	7.14	46.81	6.83	95.61%	93.33%	46.78%
ZJ-GZ-2	50.61	7.59	49.78	7.27	95.78%	93.93%	47.12%
ZJ-GZ-3	50.87	7.63	50.07	7.33	96.01%	94.54%	46.88%
ZJ-GZ1-1	48.1	7.22	47.34	6.91	95.76%	94.48%	47.47%
ZJ-GZ1-2	50.47	7.57	49.78	7.27	96.04%	94.66%	47.56%
ZJ-GZ1-3	49.77	7.47	49	7.14	95.59%	90.81%	47.56%

KEGG enrichment analysis of DEGs in liver and brain tissues identified 247 and 240 signaling pathways, respectively, 68 and 53 of which were significantly altered at high temperatures. The pathway items with more than two DEGs were screened and sorted in descending order according to their -log10 P value. The top 20 bubbles in the KEGG enrichment analysis are shown in Fig. 5. In liver tissues, the DEGs between the ZJ-GZ1 and ZJ-GZ groups were mainly enriched in the cAMP signaling pathway (ko04024, 50 genes), apoptosis (ko04210, 30 genes), and pancreatic secretion (ko04972, 27 genes). Between the ZJ-N1 and ZJ-N groups of the liver tissue, DEGs were mainly enriched in the calcium signaling pathway (ko04020, 37 genes), MAPK signaling pathway (ko04010, 31 genes), and cGMP-PKG signaling pathway (ko04022, 22 genes).

Quantitative Real-time PCR Validation

To verify the accuracy of the transcriptome sequencing, 12 randomly selected DEGs from brain and liver tissues were

Table 3 Number of genes detected in each sample

| Sample	Gene number
ZJ-N1-1	27084
ZJ-N1-2	26954
ZJ-N1-3	26989
ZJ-N-1	26315
ZJ-N-2	26330
ZJ-N-3	26205
ZJ-GZ1-1	22242
ZJ-GZ1-2	22082
ZJ-GZ1-3	22859
ZJ-GZ-1	22090
ZJ-GZ-2	23803
ZJ-GZ-3	23201

used for validation. A comparison of the results between qRT-PCR and RNA-Seq for these DEGs was obtained. The expression patterns identified using qRT-PCR for all tested genes were in agreement with the Illumina RNA-Seq data (Fig. 6). This confirmed that the results of the RNA-Seq were accurate and could be trusted.

Discussion

In aquatic ectotherms, changes in temperature have profound effects on physiology, metabolism, and behavior (Clarke and Johnston 1999). In this study, we identified DEGs and pathways involved in high-temperature stress through the transcriptome analysis of grass carp brain and liver tissues. We found that high temperature affected multiple metabolism-related pathways, such as lipid metabolism, insulin resistance, and peroxisome proliferator-activated receptor (PPAR) signaling. This suggested that high temperature stress-related genes were involved in multiple biological processes.

Water temperature is the most relevant abiotic factor influencing lipid metabolism in teleost species (Tocher 2003). Lipid metabolism is a complex physiological process. The dysregulation of lipid metabolism can cause a variety of metabolic diseases, such as obesity, metabolic syndrome, type 2 diabetes, and cardiovascular disease (Srivastava et al. 2014; Wang et al. 2013). These diseases seriously threaten the organism's health (Xiaoli and Yang 2013). A previous study by Tzab et al. (2021) showed that lipid metabolism plays an active role in the turbot response to high-temperature stress. Turbot maintain lipid metabolism by regulating genes and metabolites associated with lipid metabolism, maintaining membrane balance, and inhibiting lipid deposition, thus relieving the deterioration in meat quality caused by high-temperature stress (Tzab et al. 2021). The stability of lipid metabolism is regulated by multiple signaling pathways, and

(a)

(b)
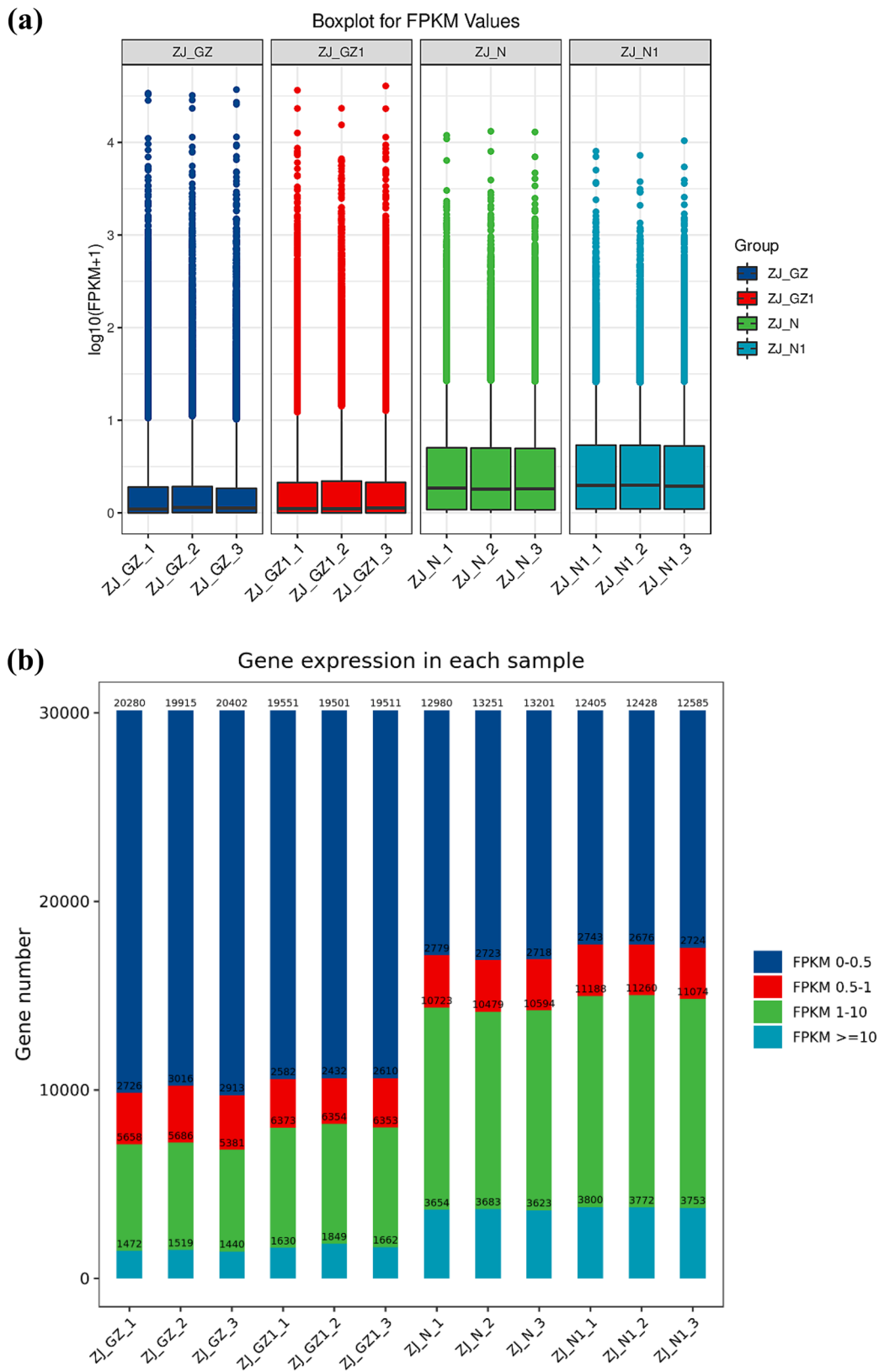
Fig. 1 **a** Boxplot of the FPKM value of each sample gene. The horizontal axis is the sample name and the vertical axis is log10(FPKM+1). The box plot for each region corresponds to five statistics (maximum, third quartile, median, first quartile, and minimum). **b** Distribution of FPKM expression. The horizontal axis is the sample, and the vertical axis is the number of protein-coding genes
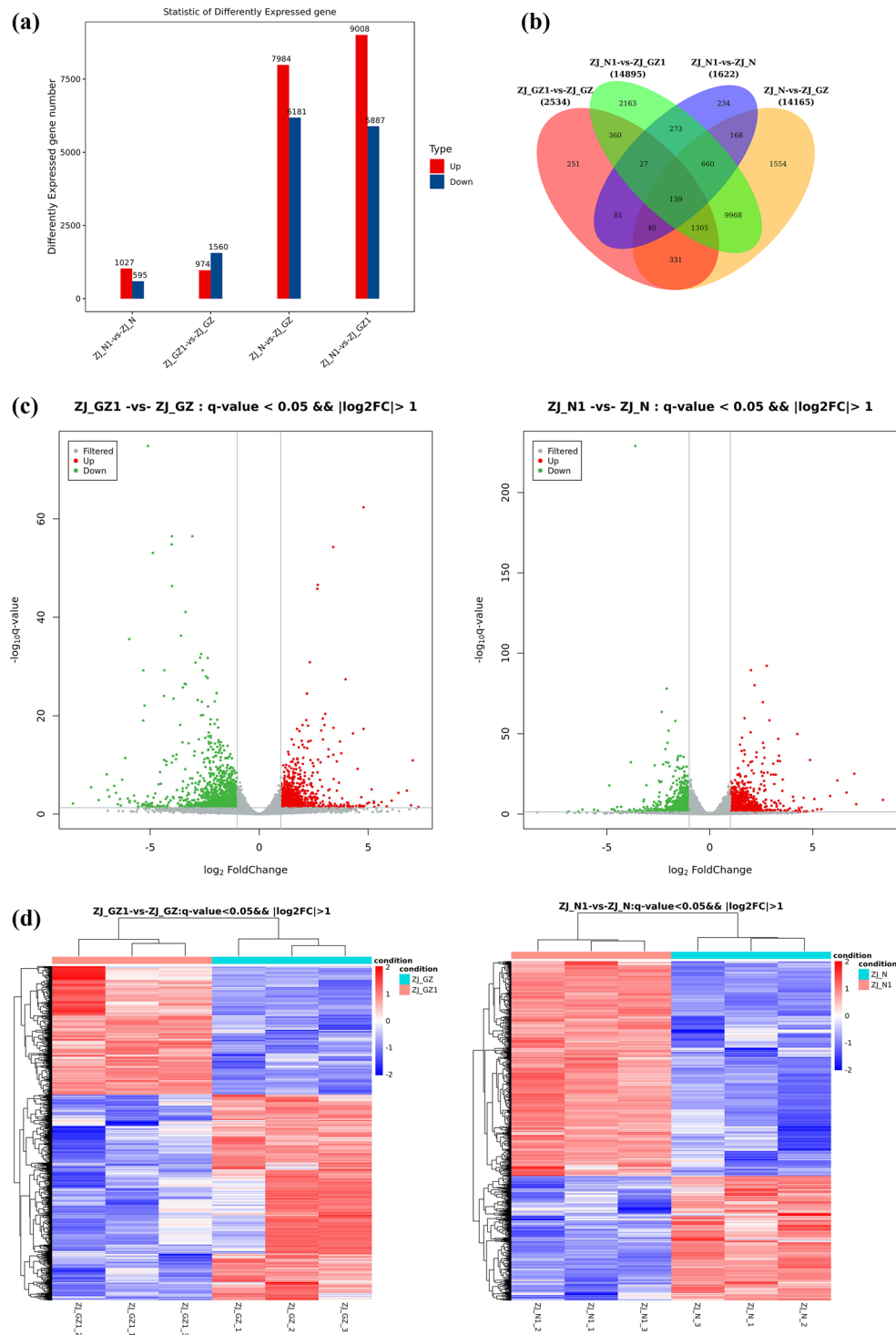
Fig. 2 a Statistical histogram of differentially expressed genes (DEGs) between the high-temperature treatment group (ZJ-GZ1, ZJ-N1) and the control group (ZJ-GZ, ZJ-N) in the liver and brain tissues. The comparison groups are on the horizontal axis; the vertical axis is the number of differentially expressed genes in the comparison group, where Up is the number of significantly differentially expressed upregulated genes and Down is the number of significantly differentially expressed downregulated genes. **b** Venn diagrams showing the overlap of DEGs among common and unique differentially expressed genes among different comparison groups. **c** Volcano maps of DEGs between the high-temperature treatment group (ZJ-GZ1, ZJ-N1) and the control group (ZJ-GZ, ZJ-N) in the liver and brain tissues. Gray indicates non-significantly different genes, red and green are significantly different genes. The horizontal axis is log2Fold-Change, and the vertical axis is -log10q-value. **d** Heat map of DEGs in ZJ-GZ1 vs ZJ-GZ, ZJ-N1 vs ZJ-N, red represents the protein-encoding genes with relatively high expression and blue represents the protein-encoding genes with relatively low expression

(a)

(b)
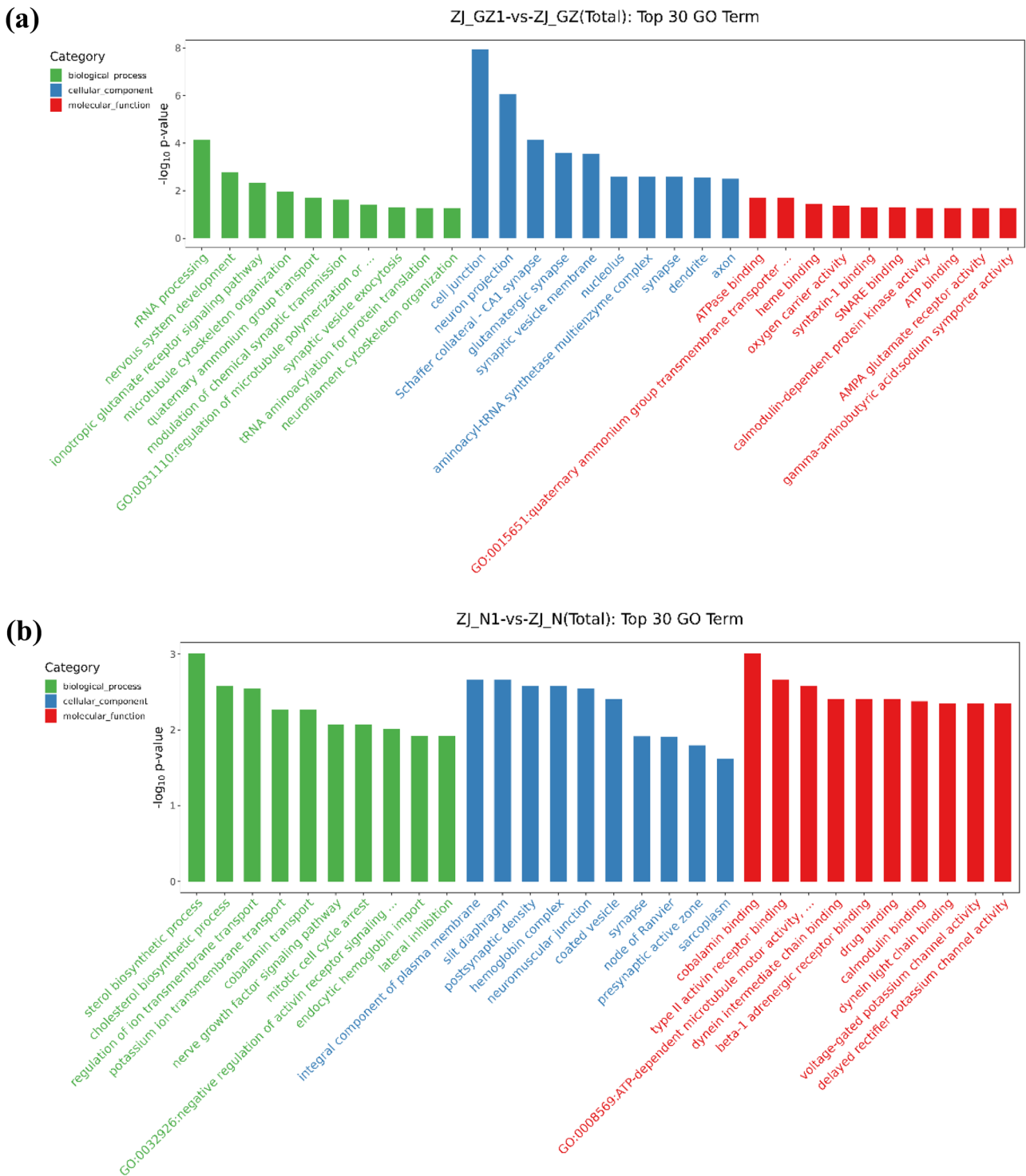
Fig. 3 GO enrichment analysis of the top 30 terms in ZJ-GZ1-vs-ZJ-GZ (**a**) and ZJ-N1-vs-ZJ-N (**b**), the horizontal axis is the GO entry name and the vertical axis is -log10 *p*-value

the signaling pathway centered on PPAR plays an important role in the regulation of lipid metabolism (Bionaz and Loor 2011). Aquaporins (AQP) are a family of transmembrane protein channels that facilitating the permeation of

water and small solutes. For example, glycerol, across cell membranes, are recognized as important players in fat metabolism (Agre 2004; Verkman 2005; Lopes et al. 2018). In our study, the FATP and AQP7 genes, which are related to lipid

(a)

(b)
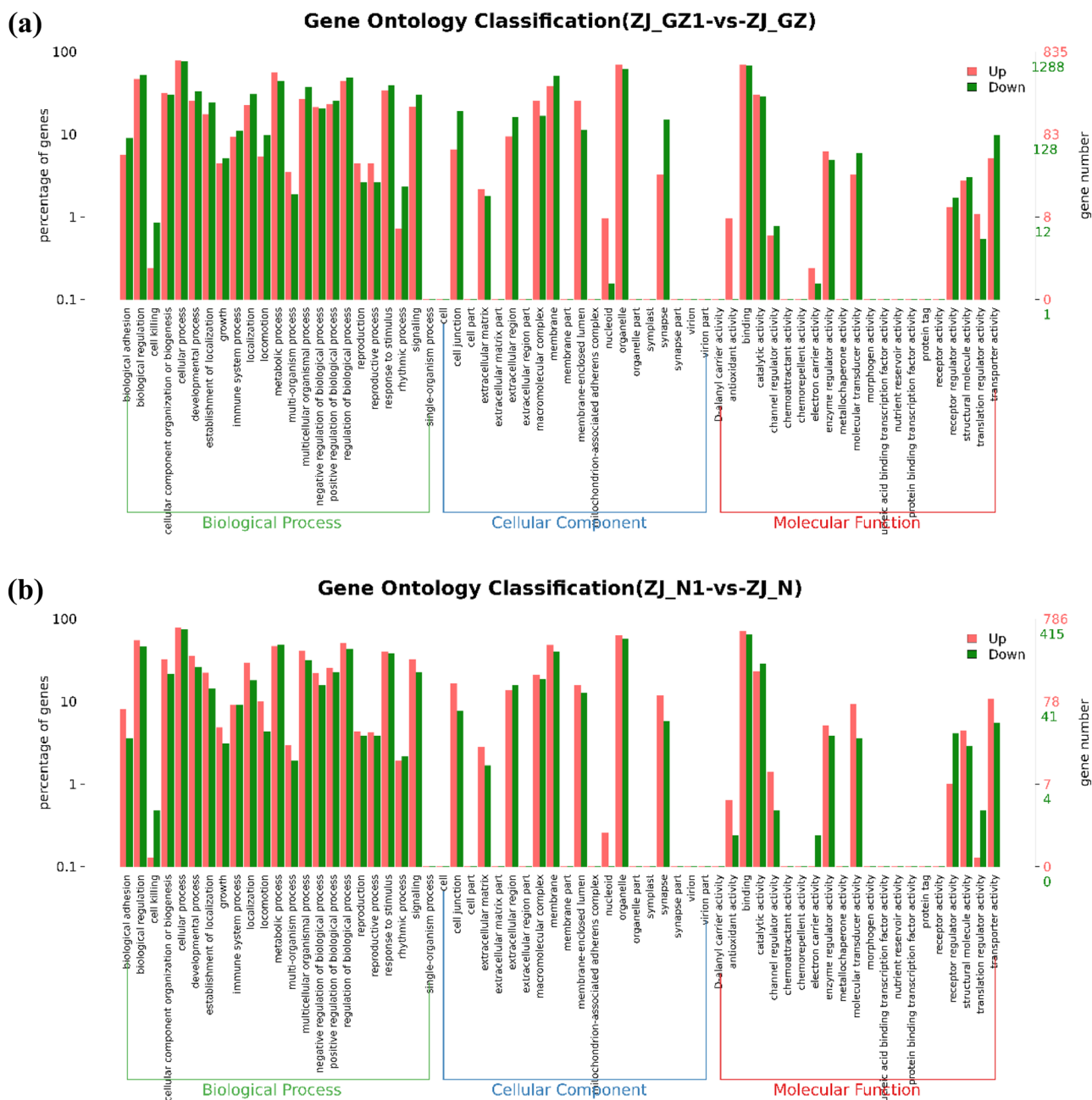
Fig. 4 Comparison of upregulated and downregulated differential genes at GO Level 2 in ZJ-GZ1 vs ZJ-GZ (**a**) and ZJ-N1 vs ZJ-N (**b**). Red represents the GO level 2 entry enriched with upregulated differentially expressed genes and green represents the GO level 2 entry enriched with downregulated differentially expressed genes. The horizontal axis represents the entry name, and the vertical axis represents the number and percentage of genes corresponding to the entry

metabolism in the PPAR signaling pathway, were significantly upregulated under high-temperature stress (Fig. 7a). We hypothesized that high temperature upregulated fatty acid metabolism by increasing the expression of FATP and affected lipid metabolism by increasing the expression of the AQP7 gene.

Apoptosis is a process of programmed cell death that plays an important role in cell development and the host immune system. Meanwhile, it is an integral component of various cellular processes that mediating phagocytosis to remove dying or infected cells (Li et al. 2015; Luo et al. 2017), preventing autoimmunity (Chen et al. 2006), and remodeling sites of

(a)

(b)
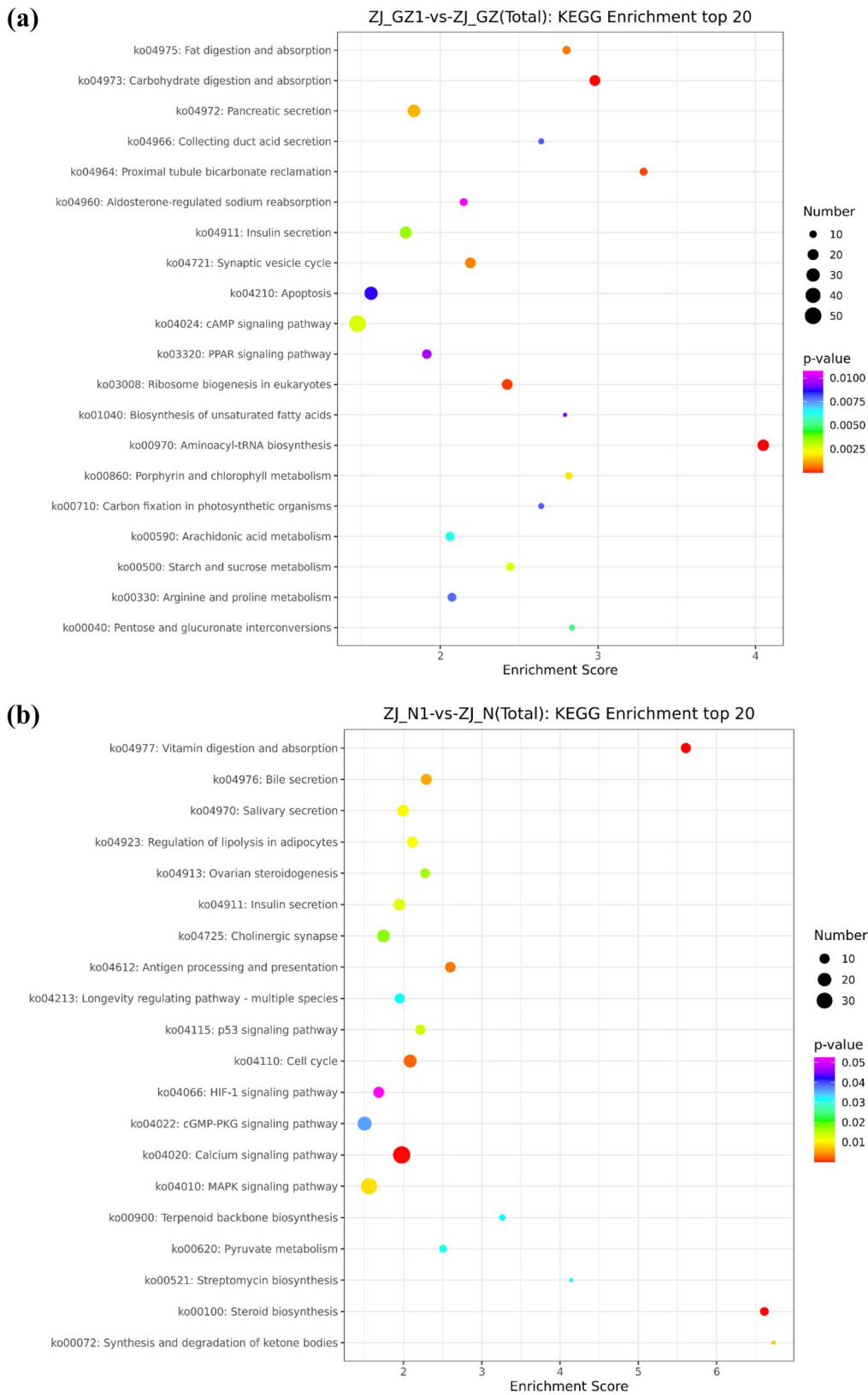
Fig. 5 KEGG analysis of the first 20 enriched pathways in bubble graphs for ZJ-GZ1 vs. ZJ-GZ (**a**) and ZJ-N1 vs. ZJ-N (**b**). The x-axis represents the enrichment score: the larger the bubble, the greater the number of DEGs. The color of the bubble changes from purple to blue to green to red, and the smaller the enrichment P value, the greater the significance
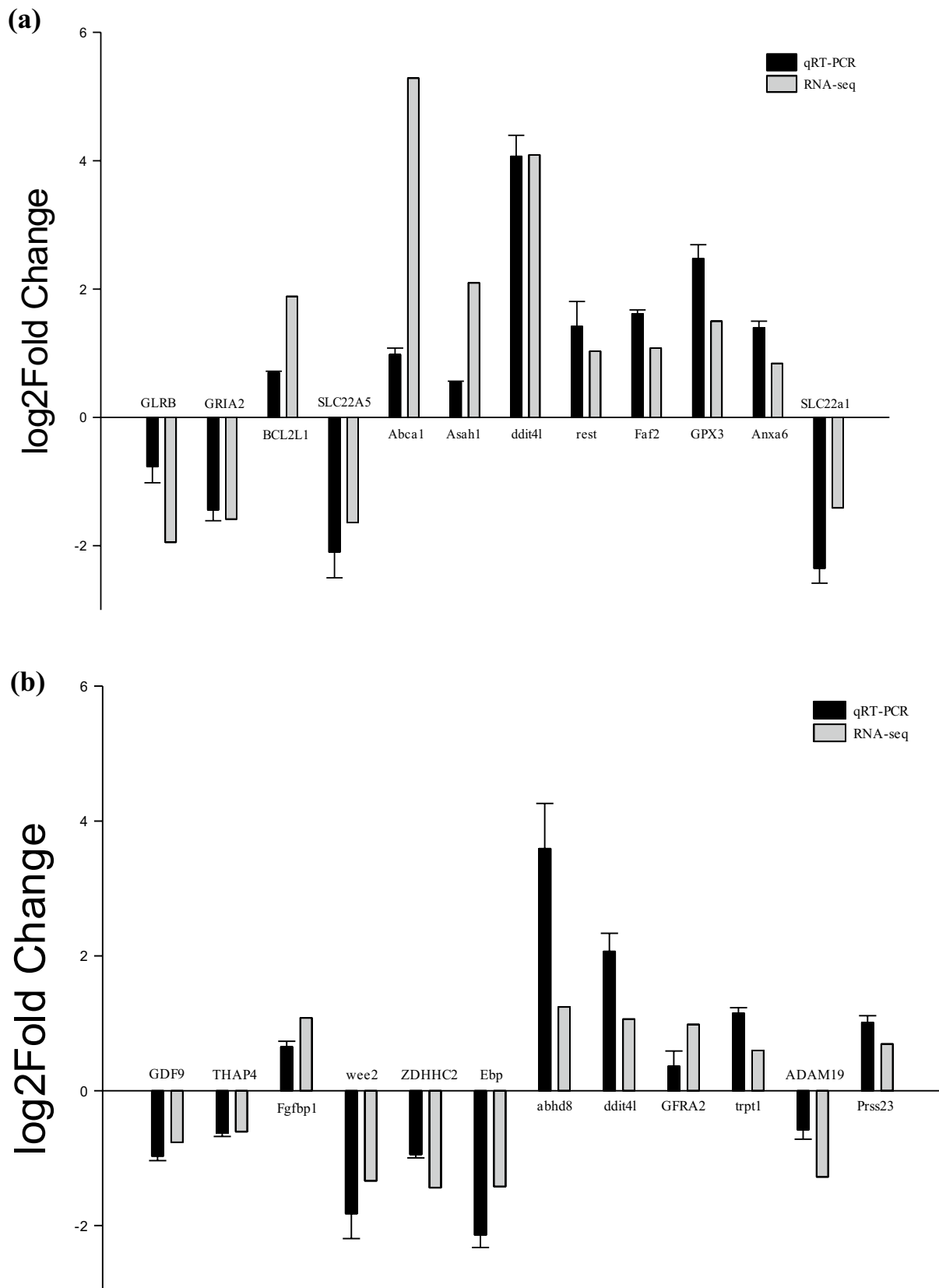
Fig. 6 Comparison of gene expression patterns obtained using comparative transcriptome analysis and qRT-PCR in liver (**a**) and brain (**b**) tissues. The transcript expression levels of the selected genes were each normalized to that of the 18 s gene

Fig. 7 Significantly differentially expressed genes identified by KEGG in the PPAR signaling pathway (**a**), apoptosis (**b**), and protein processing in the endoplasmic reticulum (**c**). Red indicates significantly upregulated genes, green indicates significantly downregulated genes, and yellow indicates genes that were both upregulated and downregulated. The red box indicates the genes discussed in the discussion section
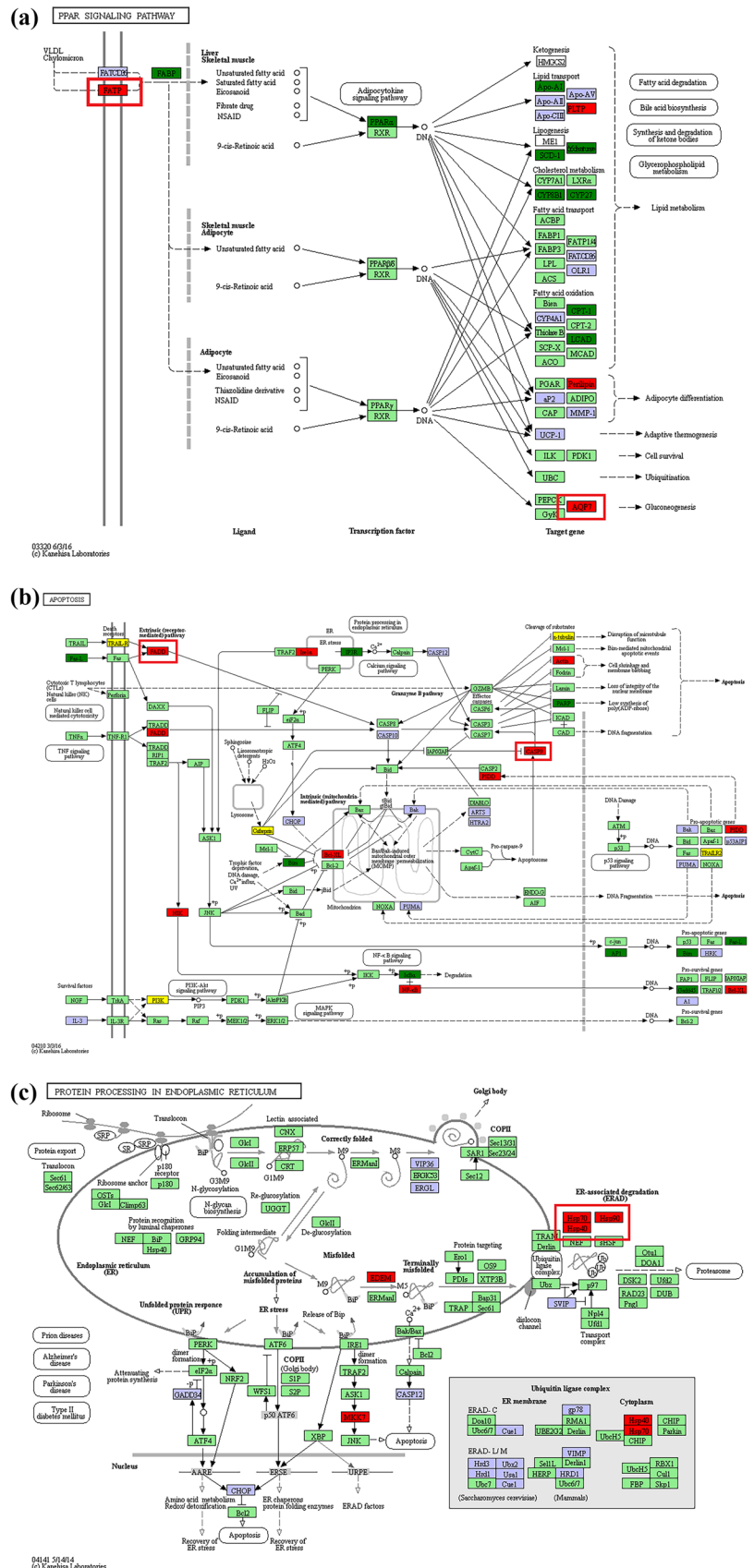
inflammation by inhibiting the release of pro-inflammatory cytokines (Savill 1997). Previous studies have found that a high-temperature challenge could increase endogenous reactive oxygen species (ROS) in aquatic organisms (Madeira et al. 2013; Li et al. 2015). The overproduction of ROS can also trigger apoptosis. High temperature-induced oxidative stress may cause apoptosis in pufferfish blood cells, and cooperatively activate the p53-Bax and caspase-dependent apoptotic pathway (Li et al. 2015). Caspases are a family of cysteine proteases that play an important role in both extrinsic and intrinsic pathways and are associated with apoptosis (Budihardjo et al. 1999). Cheng et al. (2018) found that thermal stress induced caspase-9 and caspase-3 activities in pufferfish, suggesting that the caspase-dependent pathway was playing an important role in thermal stress-induced apoptosis in fish (Cheng et al. 2018). Fas-associated protein with Death Domain (FADD) is closely associated with cell death and plays a key role in hematopoiesis, cell cycle regulation, embryogenesis, and innate immune signaling (Lu et al. 2021). In our study, Casp9 and FADD genes were significantly upregulated in the apoptotic signaling pathway under high temperatures (Fig. 7b). This indicated that the Casp9 and FADD genes played important roles in thermal stress-induced apoptosis.

The endoplasmic reticulum (ER) has important functions in intracellular calcium homeostasis, modifications, transport, and protein synthesis and folding (Naidoo 2009; Krebs et al. 2015). Stress conditions, including heat stress, oxidative stress, or inflammation, can lead to protein denaturation or misfolding, thereby reducing protein function. When an organism is stressed, many enzymes and proteins are structurally and functionally altered, and the organism then stimulates the synthesis of heat stress proteins to protect itself against adversity (Liu S et al. 2013, Parsell and Lindquist 1993). HSPs are a class of molecular chaperones that play an important role in hematopoiesis and protein metabolism (Bukau et al. 1998; Kregel 2002). The HSP family contributes not only to the correct folding of denatured proteins but also to the removal of unfolded damaged proteins (Wang et al. 2015). In a previous study, elevated water temperature increased the expression of Hsp90 and Hsp70 (Cheng et al. 2015; Cui et al. 2013). In our study, we found that high-temperature stress increased the expression of Hsp70, Hsp90, and Hsp40 in brain tissue (Fig. 7c). Among all the HSPs, Hsp40 was the largest HSP family and binded to the Hsp70 ATPase domain in assisting protein folding (Song et al. 2014). The significant upregulation of heat-stimulated proteins HSP70 and HSP90, as well as HSP40, indicated the property of heat-stimulated proteins to stimulate expression when subjected to high-temperature stress. These chaperone proteins interacted with denatured proteins to prevent their aggregation and misfolding and may enable grass carp to avoid the potential damage from high temperatures.

In conclusion, our transcriptome analysis of liver and brain tissues of grass carp under persistent high temperature stress clarified the DEGs and important pathways involved in relevant regulatory processes, which included enhanced lipid metabolism, reduced fatty acid synthesis, disrupted immune system, and increased HSP expression. The reliability of the transcriptome sequencing results was verified by real-time fluorescence quantitative PCR, and these results laid the foundation for the subsequent analysis of grass carp in response to high-temperature stress.

Declarations

References

Agre P (2004) Aquaporin water channels (Nobel Lecture) (p 4278–4290). Angew Chem Int Ed 43:4278–4290

Anders S, Pyl PT, Huber W (2015) HTSeq-a Python framework to work with high-throughput sequencing data. Bioinformatics 166–169

Bing LSS, Jian Z, Su Y, Zhang, W, Ge X (2019) Transcriptome profiling and histology changes in juvenile blunt snout bream (*Megalobrama amblycephala*) liver tissue in response to acute thermal stress. Genomics 111:242–250

Bionaz M, Loor J (2011) Gene Networks driving bovine mammary protein synthesis during the lactation cycle. Bioinform Biol Insights 5:83–98

Bo L, Xie J, Ge X, Xu P, Wang A, He Y, Zhou Q, Pan L, Chen R (2010) Effects of anthraquinone extract from Rheum officinale Bail on the growth performance and physiological responses of *Macrobrachium rosenbergii* under high temperature stress. Fish Shellfish Immunol 29:49–57

Bolger AM, Marc L, Bjoern U (2014) Trimmomatic: a flexible trimmer for Illumina sequence data. Bioinformatics 30:2114–2120

Brett JR (2015) Energetic Responses of salmon to temperature. a study of some thermal relations in the physiology and freshwater ecology of sockeye salmon (*Oncorhynchus nerkd*). Am Zool 11:99–113

Budihardjo IB, Oliver H, Lutter M, Luo X, Wang XD, Budihardjo I, Oliver H, Lutter M, Luo X, Wang XD (1999) Biochemical pathways of caspase activation during apoptosis. Annu Rev Cell Dev Biol 15:269–290

Bukau B, Horwich AL, Bakau B (1998) The Hsp70 and Hsp60 review chaperone machines. Cell 92:351–366

Chen M, Wang Y, Huang L, Sandoval H, Liu Y, Wang J (2006) Dendritic cell apoptosis in the maintenance of immune tolerance. Science 311:1160–1164

Cheng C, Yang F, Liao S, Miao Y, Ye C, Wang A, Tan J, Chen X (2015) High temperature induces apoptosis and oxidative stress in pufferfish (*Takifugu obscurus*) blood cells. J Therm Biol 53:172–179

Cheng C, Guo Z, Luo S, Wang A (2018) Effects of high temperature on biochemical parameters, oxidative stress, DNA damage and apoptosis of pufferfish (*Takifugu obscurus*). Ecotoxicol Environ Saf 150:190–198

Clarke A, Johnston NM (1999) Scaling of metabolic rate with body mass and temperature in teleost fish. J Anim Ecol 68:893–905

Cui Y, Liu B, Xie J, Xu P, Zhang Y (2013) The effect of hyperthermia on cell viability, oxidative damage, and heat shock protein expression in hepatic cells of grass carp (*Ctenopharyngodon idellus*). J Therm Biol 40:721–729

Edenhofer PR, Sokona Y, Farahani E, Kadner S, Seyboth K, Adler A, Baum I, Brunner S (2014) IPCC, 2014: Climate Change 2014: mitigation of climate change. Contribution of Working Group III to the Fifth Assessment Report of the Intergovernmental Panel on Climate Change 15:1435

Guo J, Zhang M, Wang S, Xu X, Shen Y, Li J (2022) A high-density genetic linkage map and QTL mapping for growth related traits in grass carp (*Ctenopharyngodon idella*). Aquaculture 552:738041

Handeland SO, Imsland AK, Stefansson SO (2008) The effect of temperature and fish size on growth, feed intake, food conversion efficiency and stomach evacuation rate of Atlantic salmon post-smolts. Aquaculture 283:36–42

Huey RB, Stevenson RD (2015) Integrating Thermal Physiology and Ecology of Ectotherms: A Discussion of Approaches. Am Zool 19:357–366

Huang J, Li Y, Liu Z, Kang Y, Wang J (2018) Transcriptomic responses to heat stress in rainbow trout *Oncorhynchus mykiss* head kidney. Fish Shellfish Immunol 82:32–40

Huang DY, Ren MC, Liang HL, Ge XP, Xu H, Wu LH (2022) Transcriptome analysis of the effect of high-temperature on nutrient metabolism in juvenile grass carp (*Ctenopharyngodon idellus*). Gene 809:146035

Iranshahi F, Faramarzi M, Kiaalvandi S (2011) The Effect of probiotics on growth performance and body composition of common carp (*Cyprinus carpio*). J Anim Vet Adv 10:2408–2413

Jeffries KM, Hinch SG, Sierocinski T, Pavlidis P (2013) Transcriptomic responses to high water temperature in two species of Pacific salmon. Evol Appl 7:286–300

Kim D, Langmead B, Salzberg SL (2015) HISAT: a fast spliced aligner with low memory requirements. Nat Methods 12:357-U121

Krebs J, Agellon LB, Michalak M (2015) Ca2+ homeostasis and endoplasmic reticulum (ER) stress: an integrated view of calcium signaling. Biochem Biophys Res Commun 460:114–121

Kregel KC (2002) Invited Review: Heat shock proteins: modifying factors in physiological stress responses and acquired thermotolerance. J Appl Physiol 192:2177–2186

Li AJ, Leung P, Bao V, Lui G, Leung K (2015) Temperature-dependent physiological and biochemical responses of the marine medaka Oryzias melastigma with consideration of both low and high thermal extremes. J Therm Biol 54:98–105

Liu F, Wang D, Fu J, Sun G, Shen Y, Dong L, Zhang B, Hu S, Li J (2010) Identification of immune-relevant genes by expressed sequence tag analysis of head kidney from grass carp (*Ctenopharyngodon idella*). Comp Biochem Physiol Part D Genomics Proteomics 5:116–123

Liu S, Wang X, Sun F, Zhang J, Feng J, Liu H, Sun Y, Zhang Y, Liu Z (2013) RNA-Seq reveals expression signatures of genes involved in oxygen transport, protein synthesis, folding, and degradation in response to heat stress in catfish. Physiol Genomics 45:462–476

Lopes PA, Martins R, Silva I, Madeira MS, Prates J, Soveral G (2018) Modulation of aquaporin gene expression by n-3 long-chain PUFA lipid structures in white and brown adipose tissue from hamsters. Br J Nutr 120:1098–1106

Love MI, Huber W, Anders S (2014) Moderated estimation of fold change and dispersion for RNA-seq data with DESeq2. Genome Biol 15:550

Lu Z, Tang M, Li Y, Shi F, Zhan F, Zhang M, Zhao L,Li J,Lin L,Qin Z(2021) Molecular cloning and characterization of FADD from the grass carp (*Ctenopharyngodon idellus*) in response to bacterial infection. Aquaculture 542:736829

Luo SW, Kang H, Kong JR, Xie RC, Liu Y, Wang WN, Xie FX, Wang C, Sun ZM (2017) Molecular cloning, characterization and expression analysis of (B-cell lymphoma-2) Bcl-2 in the orange-spotted grouper (*Epinephelus coioides*). Dev Comp Immunol 76:150–162

Madeira D, Narciso L, Cabraln HN, Vinagre C, Diniz MS (2013) Influence of temperature in thermal and oxidative stress responses in estuarine fish. Comp Biochem Physiol a: Mol Integr Physiol 166:237–243

Mahanty A, Mohanty S, Mohanty BP (2017) Dietary supplementation of curcumin augments heat stress tolerance through upregulation of nrf-2-mediated antioxidative enzymes and hsps in Puntius sophore. Fish Physiol Biochem 43:1131–1141

Naidoo N (2009) ER and aging—Protein folding and the ER stress response. Ageing Res Rev 8:150–159

Parsell DA, Lindquist S (1993) The function of heat-shock proteins in stress tolerance: degradation and reactivation of damaged proteins. Annu Rev Genet 27:437–496

Roberts A, Trapnell C, Donaghey J, Rinn JL, Pachter L (2011) Improving RNA-Seq expression estimates by correcting for fragment bias. Genome Biol 12:1–14

Sangwan RS, Tripathi S, Singh J, Narnoliya LK, Sangwan NS (2013) De novo sequencing and assembly of *Centella asiatica* leaf transcriptome for mapping of structural, functional and regulatory genes with special reference to secondary metabolism. Gene 525:58–76

Savill J (1997) Apoptosis in resolution of inflammation. J Leukoc Biol 61:375–380

Shen Y, Wang L, Fu J, Xu X, Yue GH, Li J (2019) Population structure, demographic history and local adaptation of the grass carp. BMC Genomics 20:467

Shen Y, Yue G (2018) Current status of research on aquaculture genetics and genomics-information from isga 2018. Aquac Fish 4:43–47

Song L, Zhang J, Li C, Yao J, Jiang C, Li Y, Liu S, Liu Z (2014) Genome-wide identification of Hsp40 Genes in channel catfish and their regulated expression after bacterial infection. PLoS ONE 9:0115752

Srivastava SP, Shi S, Koya D, Kanasaki K (2014) Lipid mediators in diabetic nephropathy. Fibrogenesis & Tissue Repair 7:12–12

Sun S, Wu Y, Yu H, Su Y, Ren M, Zhu J, Ge X (2018) Serum biochemistry, liver histology and transcriptome profiling of bighead carp *Aristichthys nobilis* following different dietary protein levels. Fish Shellfish Immunol 86:832–839

Tocher DR (2003) Metabolism and functions of lipids and fatty acids in teleost fish. Rev Fish Sci 11:107–184

Tzab C, Amb C, Syb C, Zhb C (2021) Integrated metabolome and transcriptome analyses revealing the effects of thermal stress on lipid metabolism in juvenile turbot *Scophthalmus maximus*. J Therm Biol 99:102937

Verkman AS (2005) More than just water channels: unexpected cellular roles of aquaporins. J Cell Sci 118:3225

Verma AK, Pal AK, Manush SM, Das T, Dalvi RS, Chandrachoodan PP, Ravi PM, Apte SK (2007) Persistent sub-lethal chlorine exposure augments temperature induced immunosuppression in *Cyprinus carpio* advanced fingerlings. Fish Shellfish Immunol 22:547–555

Wang F, Dai AY, Tao K, Xiao Q, Huang ZL, Gao M, Li H, Wang X, Cao WX, Feng WL (2015) Heat shock protein-70 neutralizes apoptosis inducing factor in Bcr/Abl expressing cells. Cell Signal 27:1949–1955

Wang J, Scholtens D, Holko M, Ivancic D, Lee O, Hu H, Chatterton RT, Sullivan ME, Hansen N, Bethke K (2013) Lipid metabolism

genes in contralateral unaffected breast and estrogen receptor status of breast cancer. Cancer Prev Res 6:321–330

Wang K, Li H, Xu Y, Shao Q, Yi J, Wang R (2019) MFEprimer-3.0: quality control for PCR primers. Nucleic Acids Res 47:W610-W613

Wenning R(2020). THE STATE OF WORLD FISHERIES AND AQUACULTURE (SOFIA) 2020 REPORT. Integrated Environmental Assessment and Management, 16: 800–801.

Xiao L, Yang F (2013) Mediating lipid biosynthesis: implications for cardiovascular disease. Trends Cardiovasc Med 23:269–273

Yang Y, Yu H, Li H, Wang A, Yu HY (2016) Effect of high temperature on immune response of grass carp (*Ctenopharyngodon idellus*) by transcriptome analysis. Fish Shellfish Immunol 58:89–95

Zhao S, Guo S, Zhu Q, Yuan S, Zheng J (2017) Heat-induced oxidative stress and inflammation involve in cadmium pollution history in the spleen of zebrafish. Fish Shellfish Immunol 72:1–8

Zhao T, Ma A, Huang Z, Liu Z, Sun Z, Zhu C, Yang J, Li Y, Wang Q, Qiao X, Chen Z (2021) Transcriptome analysis reveals that high temperatures alter modes of lipid metabolism in juvenile turbot (*Scophthalmus maximus*) liver. Comp Biochem Physiol d: Genomics Proteomics 40:100887

Zhi Z, Liu Z, Wang LG (2019) Oxidative stress, apoptosis activation and symbiosis disruption in giant clam Tridacna crocea under high temperature. Fish Shellfish Immunol 84:451–457

Zhou Z, Li Y, Zhang G, Ye H, Luo J (2020) Effects of temperature on the transcriptomes of pituitary and liver in Golden Pompano *Trachinotus blochii*. Fish Physiol Biochem 46:63–73